Ferroelectricity in Water Ice

M. J. Iedema,*,† M. J. Dresser,‡ D. L. Doering,§ J. B. Rowland,† W. P. Hess,† A. A. Tsekouras,†,|| and J. P. Cowin†

Pacific Northwest National Laboratory, Box 999, M/S K8-88, Richland, Washington 99352, Department of Physics, Washington State University, Pullman, Washington 99163, and Associated Western Universities, Richland, Washington 99352

Received: June 9, 1998; In Final Form: September 4, 1998

Partially proton-ordered ice I (cubic) was grown from the vapor phase, from 40 to nearly 150 K. It is believed to be metastable and oriented by the asymmetry of the solid−vacuum interface during growth. This was studied using a Kelvin (work function) probe for ice grown on a single-crystal Pt(111) substrate. The ice grows with a slight preference for the O-end aimed away from the surface, with about 0.2% net up dipole per water molecule at 40 K, or about −3 mV/monolayer of deposited ice film. This decreases with deposition temperature as exp(−*T*/27 K). Near 130, 140, and 150 K sharp features occur as the ice changes from amorphous to crystalline, and dielectric properties become active. By 150 K the effect seems to be zero. These results are discussed in context with other recent reports on ferroelectric ice. In addition to influencing several kinds of vacuum-based studies of ice, this slight ferroelectricity may allow natural ice vapor-grown in space to develop large electric fields.

Introduction

Water ice is well-known to have a simple tetrahedral arrangement of hydrogen bonds between the oxygen of one water and a hydrogen from each of two adjacent water molecules. While maintaining this bonding arrangement, it is still possible to arrange the orientations of the water dipole in nearly endless periodic or nonperiodic arrangements, which are thermally populated for ice above 160 K or so. Below this, a proton-ordered phase may be the most stable form, but this has never been observed, as the kinetics of proton reorientation become too slow before any transition can be reached. Thus the elusive proton-ordered "normal" ice (ice I) has held a long fascination with researchers.

The energy differences between proton-disordered and proton-ordered (including antiferroelectric and ferroelectric) forms of ice are small and not easy to calculate. A recent work by Lekner[1] calculated water electrostatics for protons. He found, for superlattice unit cells of 8−16 water molecules, that the lowest energy state was antiferroelectric, with the energy growing quadratically with the net unit cell dipole. However, the energy differences were millielectronvolts, and the entropy was highest for "weakly ferroelectric" unit cells. For this reason, proton-ordered ice is not expected to be thermodynamically stable except at temperatures well below 100 K,[2] where *kT* would become less than the energy differences. To create proton-ordered ice I, it might be reasonable to do so by "tricks", such as (a) growing ice at low temperatures on a substrate that forces a proton order on the film, (b) using the asymmetry of the vapor−ice interface to orient growing ice, (c) making ice I from a proton-ordered high-pressure form of ice, (d) catalyzing the orientational flipping by doping or injecting from an interface ions or hydrogen-bond defects, or (e) growing the ice in the presence of an applied field. These ideas have been around for a long time and have been tried more than once (and have usually clearly failed). Some methods clearly would create metastable systems at best using templating or kinetic tricks. But, if successful, they can create valid bulk systems, just as people make real diamond at room temperature via thin film methods at room temperature. Some recent papers (including this one) have claimed some success at growing bulk-aligned ice I's.

Ferroelectric ice has recently been reported by Su et al.,[3] as vapor grown on Pt(111). They used laser sum frequency generation to detect optically the asymmetry in water ice and the ice−Pt(111) interface. Sum frequency generation requires a loss of inversion symmetry, so it is seen primarily for molecules in the few angstroms around the interface between two phases, while bulk liquids usually provide zero signal. They expect a preference for H end up (or down) at the ice−Pt interface to force a net proton-order in a growing ice film. They found a ferroelectric ordering in the growing film that behaved as if it were "strong" only for the first 20 monolayers, for water ice they grew from 120 to 137 K. At such high temperatures, it is not likely that a bulk phase of proton-ordered ice exists in equilibrium. One might reasonably hope to generate a metastable phase, or even a thin, stable, Pt-interface-stabilized "interphase" with proton order. Unfortunately, they did not analyze their results to determine if the polarization was complete (all water molecules oriented, or some tiny fraction). This is an important issue that our results help resolve.

Proton-ordered ice I, where the transition has been catalyzed by dopents or impurities, has been reported by several workers, from the 1960's[4] to more recent work.[5,6] In the latter case, the suspected proton-ordered ice has been labeled "ice XI", though this is meant to designate a particular proton-ordered form of ice I. Much of the evidence has been from the electrical and heat capacity behavior, though neutron diffraction has been

† Pacific Northwest National Laboratory.
‡ Washingotn State University.
§ Associated Western Universities.
|| Currently at Laboratory of Physical Chemistry, University of Athens, Athens, GR-15771, Greece.

10.1021/jp982549e CCC: $15.00
Published on Web 10/22/1998

recently used to assist in the identification.[7] Johari and Jones[8] discussed the earlier work[4] thoroughly and concluded they were *not* observing proton-ordered ice phases, but simply properties expected from the known sluggish polarization kinetics of the ice. We will similarly (though much less thoroughly) examine the more complex case of ice XI.

The most direct way to measure the *ferroelectric* proton ordering of ice is to measure the electric potential difference across a film caused by its polarization. We have done this by growing a thin film on a metal substrate and measuring the change in contact potential (work function) caused by the film. Here we are relying on the asymmetry of the vapor−ice interface to create the net alignment. This is a noncontact measurement and can be done with high accuracy: One can measure total potential changes from a few millivolts to thousands of volts. We measured the work function change due to ice films grown from the vapor, as a function of growth temperature and film thickness. For each growth temperature, after measuring the contact potential at the growth temperature, we ramped the temperature upward, to probe the depolarization properties. As discussed below, for low-temperature vapor deposition ($<$130 K) the ice forms an amorphous film, while above 140 K it grows crystalline. Our results show the ferroelectric effect ranges from about 1.5% dipole-aligned for growth near absolute zero (with net oxygen end up), to less than 10^{-4} % dipole-aligned for growth at 150 K.

Similar results were reported earlier: Kutzner[9] reported in 1972 on measurements of spontaneous ferroelectric ordering of vapor-grown water ice from 10 to 110 K, as well as for seven other ices grown from vapors of common polar molecules. He analyzed the results quantitatively and found that (except for N_2O) the ferroelectric ordering was at most on the order of 1% fully aligned. His results for water are in excellent agreement with our data, as we shall see. Onsager et al.[10] (published after Onsager's death) repeated the water experiment of Kutzner in a qualitative way, perhaps to allow the old master to improve upon the clarity of Kutzner's explanation.

Experimental Section

The experiments were conducted in an ultrahigh vacuum chamber with a base pressure of 2×10^{-10} Torr, which was pumped with an ion pump, assisted by cryopumping from a helium closed-cycle refrigerator. The chamber was equipped with a double-pass cylindrical mirror analyzer for Auger electron spectroscopy (AES), a McAllister Technical Services Kelvin probe for contact potential difference measurement (CPD), an Extrel quadrupole mass spectrometer for temperature-programmed desorption (TPD), a molecular beam doser, a tube doser to achieve higher coverages, and an ion gun for sputtering the Pt(111) substrate. The sample manipulator was mounted 6 in. off-center of a 24 in. rotatable top flange. The sample was moved in front of each instrument by rotating the top flange.

The 1 cm diameter Pt(111) single-crystal substrate was spot-welded to a tantalum foil (0.01 in. thickness), which was in turn mounted on a Au-coated copper fork. This was attached to a large copper piece cooled by the helium closed-cycle refrigerator. The substrate could be heated either radiatively or through electron beam bombardment by filaments mounted behind the crystal. The substrate temperature was feedback-controlled from 30 to 1600 K by this arrangement. Temperature was measured with type K (chromel/alumel) thermocouple spot-welded to the edge of the crystal, calibrated with a Si diode temperature sensor for cryogenic temperatures.

Using the Auger spectrometer to monitor the Pt surface composition, the only major contaminant observed was carbon. When flashing to 1000 K was not sufficient to remove this feature, it was cleaned by cycling the substrate temperature between 550 and 1000 K in a background pressure of 2×10^{-8} Torr oxygen. The only other contaminant we routinely saw was about 0.5% of a monolayer of indium (a remnant of In foil used in the past on the substrate holder). This would be reduced when necessary by cycles of neon sputter-annealing.

Almost all water doses were done using the tube doser. Triply distilled H_2O was put into a reservoir, where it was frozen, pumped on via turbo pump, and thawed, sequentially, for three cycles. A tube whose inner diameter was about 0.2 mm larger than the crystal was placed about 1 mm from it. Water vapor was introduced to the tube via a leak valve, and an annular baffle about 1 cm from the end of the tube prevented any capillary beaming effects and improved the uniformity of the doser. The purity of the deposition gas as it back-filled the chamber was periodically checked with the mass spectrometer. As the water film thickness was sometimes quite large, even small amounts of air remaining in the water caused some contamination problems, as will be discussed later. During dosing, the Pt(111) crystal would be brought as close as possible to the tube, to minimize the pressure load on the chamber and to avoid dosing the crystal supports. Dosing time varied roughly with the thickness of the film, in the range of 30−600 s.

Following film growth, the coated substrate was moved to the Kelvin probe position. The Kelvin probe gives the contact potential difference (CPD) between the coated substrate or "sample" and the gold-coated Kelvin probe. In the case of the clean surface, the CPD is just the difference in work function of the two materials (i.e., $\Phi_{probe} - \Phi_{sample}$, where Φ_{probe} and Φ_{sample} are the work functions of the probe and of the sample). We were able to get a stable CPD signal within 5 min, and the temperature ramp would be started at the 5 min mark. The ramps were done at 0.5 K/s up to 300 K. The substrate was then rapidly flashed to 1100 K to clean it (water is gone by 200 K, trace oxygen and carbon removal required the highest temperature).

Film thicknesses used for these experiments were generally in two ranges, either about 2000 ML or about 100 000 ML.[11] In previous experiments with thinner films, we would use our molecular beam doser, which doses at about 1 ML per 5 s. We would typically measure our coverage by first determining the dosing time to just complete the first monolayer, seen when the high temperature peak near 175 K just saturates. As the sticking probability is near 1 at all coverages, those integrals are also conveniently proportional to dose time. To make a 20 ML film, for example, we then dose 20 times longer. For the much thicker films, we needed a much more intense source, using a simple tube doser fed by a leak valve. Unfortunately this was not very reproducible in flux (±25% or more at the same leak valve setting), so we had to measure the film thickness for each run. We could not use the TPD integrals to calibrate the film thickness, as we found that our chamber pumping speed for water shows considerable saturation effects above about 30 ML desorbed. Instead, we used the temperature of the peak desorption rate, T_p, to calibrate the initial coverage θ_0. T_p is little affected by the pumping speed variations. The zeroth order TPD expression

$$\frac{d\theta}{dt} = -\frac{\nu}{\sigma_{ML}} e^{-E_a/(RT)} = \beta \frac{d\theta}{dT} \qquad (1)$$

$$T = \beta t$$

can be integrated to yield the initial coverage θ_0 as a function

of peak desorption temperature T_p, given the preexponential ν, the activation energy for desorption, E_a, and σ_{ML}, the coverage of 1 ML, 1.05×10^{15} cm^{-2}. Assuming that the temperature goes as βt, eq 1 can be converted to one for dq/dT. For an ideal zeroth order desorption, the desorption rate increases with temperature, until it abruptly ceases when all the material is gone. So the temperature of peak desorption is the temperature T_p such that if we integrate eq 1 from 0 K to T_p, the calculated change in coverage is the total initial coverage θ_0. This can be used to transform the measured T_p into the initial coverage. Actually since the first monolayer is bound much more tightly than the rest, we set the integral to $\theta_0 - 1$. Integrating eq 1 can be done by changing variables to $x = E_a/RT$ and expanding the factor $1/x^2$ that is generated as a Taylor series in $(x - x_p)$.

$$\int_0^{T_p} \mathrm{d}T \frac{\mathrm{d}\theta}{\mathrm{d}T} \equiv -(\theta_0 - 1) = -\frac{\nu}{\beta\sigma_{ML}} \int_0^{T_p} \mathrm{d}T\, \mathrm{e}^{-E_a/(RT)}$$

$$x \equiv \frac{-E_a}{RT} \Rightarrow \theta_0 - 1 = \frac{\nu E_a}{\sigma_{ML}\beta R} \int_{x_p}^{\infty} \mathrm{d}x \frac{\mathrm{e}^{-x}}{x^2}$$

$$\frac{1}{x^2} = \frac{1}{x_p^2} - \frac{2}{x_p^3}(x - x_p) - \frac{3}{x_p^4}(x - x_p)^2 - \frac{3}{x_p^4}(x - x_p)^3 \ldots \quad (2)$$

$$\Rightarrow \theta_0 = 1 + \frac{\nu R T_p^{\,2}}{\sigma_{ML}\beta E_a} \mathrm{e}^{-E_a/(RT_p)} \left(1 - \frac{2!}{\left(\frac{E_a}{RT_p}\right)} + \frac{3!}{\left(\frac{E_a}{RT_p}\right)^2} - \frac{4!}{\left(\frac{E_a}{RT_p}\right)^3} + \ldots\right)$$

The resulting expression for θ_0 contains an infinite series actually only "asymptotically converging", diverging after 30 terms. But with E_a/RT_p on the order of 30, the series expression is accurate to about 7% truncated at the first term, 0.6% with the second, and 0.07% with the third and is typically about 0.94.

We use the desorption kinetics for H_2O measured recently by Speedy et al.:[12] $\nu = 3.99 \times 10^{15}$ molecules cm^{-2} s^{-1} and $E_a = 48.25$ kJ/mol. A calculation of θ_0 as a function of T_p based on integrating eq 1 with these kinetic parameters is shown in Figure 1. This should be considered only accurate for coverages well over 1 ML. Data taken at low coverages using the molecular beam doser where the coverage was independently known is also plotted. It did not quite match this absolute curve. This is likely due to a small thermocouple calibration mismatch. To create our coverage calibration curve of θ_0 as a function of T_p, we simply translated the curve -3.5 K to match our known points, as shown in Figure 1. All coverages shown in this study were determined using this curve. Figure 2 shows a typical TPD with the Kelvin probe in position. The Kelvin probe sits very close to the coated substrate over about half its area and slows the desorption of water from the area under it, as it forces the water to return many times to the surface and reevaporate. We observed that the partial blocking by the Kelvin probe did not affect the temperature of the sharp peak from the unblocked area, and it is the peak temperature of this "unblocked" TPD peak that is used to calibrate the coverage. Comparison of TPD-peak temperature calculated coverages to beam doser coverages (up to a few hundred monolayers) showed that the TPD-peak temperature calculated coverages to be reproducible to about 3%, and similarly as accurate, over the range checkable with the molecular beam doser. We also found that at higher coverages, the ferroelectric voltages developed gave smooth and reproducible curves (to about 2%) when plotted against the TPD-peak temperature calculated coverages, despite the irreproducibility of the tube doser.

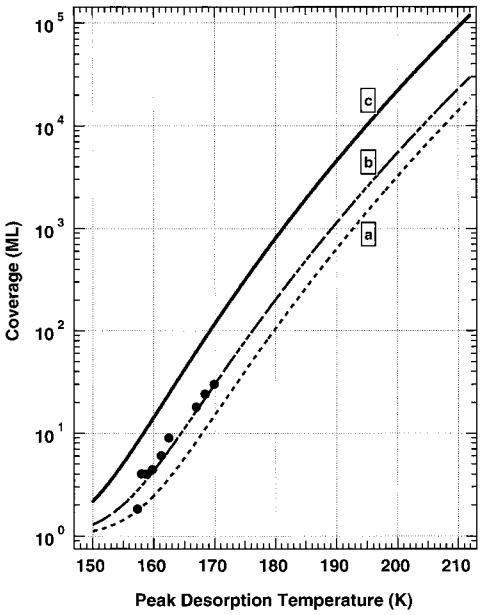

Figure 1. Coverage as a function of H_2O peak desorption temperature. The curve represented by eq 2 of the text, using a temperature ramp rate of 2 K/s, is labeled a. Dots indicate lower coverage data where the coverage was known. Trace b is the result of shifting trace a -3.5 K to overlay these data points. Trace c is the solution to eq 2 for a ramp rate of 0.5 K/s (the ramp rate used for the combination TPD/CPD runs), shifted by the temperature correction of -3.5 K.

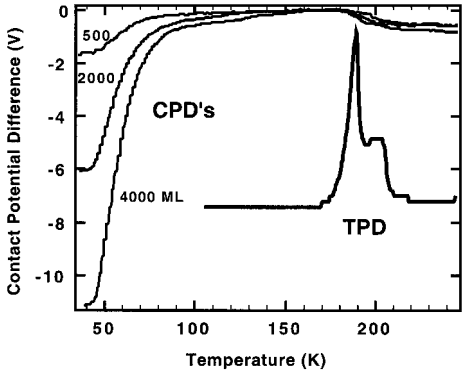

Figure 2. CPD measurements taken as the temperature is ramped (0.5 K/s) for 500, 2000 and 4000 ML (all deposited at 40 K). The temperature-programmed desorption (TPD) taken simultaneously is shown for comparison. (The tail of the TPD trace is an artifact due to the occlusion of the Kelvin probe. It is in close proximity to the coated substrate and hinders the desorption of water directly beneath it.)

Care must be taken to prevent any stray electrons or other charged particles from co-depositing on the substrate. This same apparatus is used for soft landing of ion experiments with 1 nA ion beams,[13] so we are very aware of the effects of stray currents. Generally no stray currents hit the front of the sample above a picoampere or so, too small to affect our measurements. A potential problem is the current produced by the ionizer of the quadrupole mass spectrometer. For most of the data this mass spectrometer was kept off until just before the film would begin to desorb during the ramped temperature portions of the experiments. Then the area of the sample where the Kelvin probe measures the work function would be shielded by the Kelvin probe from any external currents. For some of the earlier experiments the mass spectrometer was left on. To check whether significant current could have gotten to the front of the ice film during the brief move between the tube doser and the Kelvin probe, we repeated a few experiments with and

without the mass spectrometer on and found no difference between the unexposed and exposed samples.

To assess the crystallinity of the ice films, we studied several films by transmission Fourier transform infrared spectroscopy (FTIR). To obtain comparable results between the FTIR and TPD/CPD data, careful attention was given to match the time of film deposition, film thickness, and time of data collection. D_2O was added to an initial concentration of 1%, to increase spectral resolution (see below). It then underwent three freeze−pump−thaw cycles to purify the water. Thin films of H_2O ice were vapor-deposited onto a KBr substrate cooled to temperature between 20 and 150 K by a closed-cycle helium cryostat. An average deposition time of ∼1.5 min was required to produce an average film thickness of ∼0.5 mm (1300 ML), calculated from optical interference measurements using a 633 nm helium−neon laser.[14] Approximately 4 min after deposition, infrared spectra are obtained by a Mattson Fourier transform infrared spectrometer at a resolution of 2 cm^{-1}.

Results

Figure 2 shows the CPD data for several initial coverages, for ice grown at 40 K. Also shown is the water TPD data for one of the coverages. Note first that the CPD at the growth temperature is increasingly negative as the coverage increases. This corresponds to the work function of the Pt plus ice becoming larger, thus to polarization of the water film with the negative side toward the vacuum. We did not anticipate this ferroelectric effect when we first noticed it in the course of our soft-landed ions experiments,[13] and we immediately looked for other possible causes. The most plausible cause was some sort of stray charge incorporated within the ice. But as discussed in the Experimental Section, we eliminated this possibility. We even considered the possibility that the tube doser or molecular beam was emitting charge. We looked for any current to the sample from the two dosers during dosing. We found none (<1% of that required to create the film voltages seen). The observed ferroelectric effect was found to be reproducible over several months of work.

As the films are heated, the ferroelectric polarization disappears largely between 50 and 80 K, with traces persisting up to 100−150 K. The warmed ice layer begins to crystallize at about 160 K,[12,13] but no changes are seen in the CPD at this temperature, nor is there any coverage dependence to the CPD near that temperature. This means that by 160 K the amorphous ice is unpolarized, as is the polycrystalline ice that replaces it. Note that all the CPD data show a large shift around the end of the desorption process. This is due to the fact that the first monolayer of adsorbed water (and thus the last to leave) causes a 0.6 eV decrease in work function of the platinum surface.[15]

If the CPD shift at the deposition temperature is indeed a bulk effect, it ought to be linear with coverage. Figure 3 displays the CPD as a function of coverage. To eliminate the 0.6 eV shift caused by the first monolayer, and (as discussed later) to remove some problems caused by small contaminations, we plot the initial CPD minus that at the maximum value seen, near 176 K. The maximum value is the value at which the ferroelectric voltage has completely disappeared and all that remains is the change in work function due to the water/Pt interface. Figure 3 shows a clear linear dependence, with a bulk polarization of about −3 mV per monolayer, with no indication of any limit. The observed ferroelectricity is not an indication of a perfectly dipole-aligned ice phase but, as will be discussed later, results from a fractional percent orientation effect.

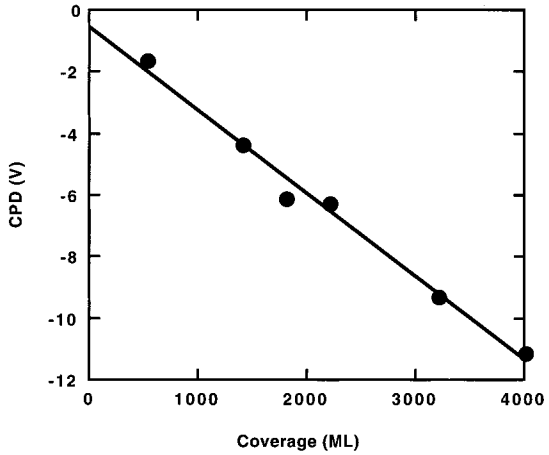

Figure 3. Change in contact potential difference (the ΔCPD) as a function of film thickness for ice films grown at 40 K, thicknesses from about 500 to 4000 ML. The linear fit has a slope of −2.69 mV/ML and an offset at zero coverage of −0.5 V.

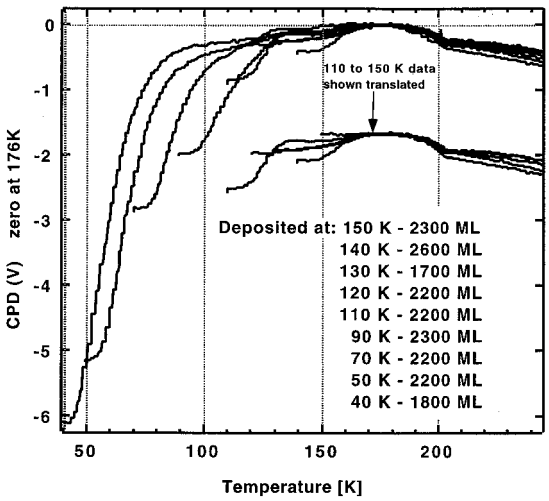

Figure 4. Comparison of the contact potential difference vs temperature curves for nearly identical ice thicknesses at different deposition temperatures (scaled per coverage to constant coverage, see text). All of the ice layers are referenced to the CPD at 176 K, approximately the maximum value. Note: the point at which the trace starts is the deposition temperature.

The dependence of the ferroelectric effect with deposition temperature *T* is different than the variation caused by ramping a coated substrate, grown at low temperature, through the same temperature *T*. Generally we would expect annealing of the amorphous ice to play a strong role, whether the coated substrate is ramped through a temperature or is grown at that temperature. However, as a film grown and measured at *T* is at that temperature for at least 5 min, while a coated substrate prepared at lower temperature and then ramped through the temperature *T* spends less than a minute near the temperature *T* (at 1/2 K/s). Thus it would be easy to suppose that films grown at higher temperatures would be more annealed than those simply ramped through that temperature. So, looking at the results in Figure 3, it would be easy to guess that the ferroelectric effect would be nearly gone for an 80 K growth temperature. This anticipation was contradicted by our results. Figure 4 shows the ΔCPD versus ramped temperature curves for several 2000 ML films, each grown at a different initial temperature.[16] Clearly the ferroelectric effect does not greatly diminish until growth temperatures around 120 K. Under most conditions the highest polarization is obtained at a given temperature by growing the film *at that temperature*.

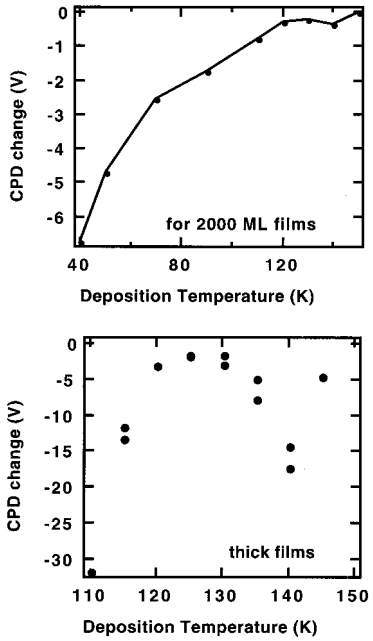

Figure 5. The ΔCPD as a function of deposition temperature, for films having nominally the same thicknesses. In (a, top), film thicknesses varied from 1800 to 2600 ML around the target thickness of 2000 ML. In (b, bottom) the thickness was more variable, with a target of 150 000 ML. Actual thicknesses follow: for deposition temperature of 110 K, 90 000 ML; 115 K, 170 000 ML and 120 000 ML; 120 K, 180 000 ML; 125 K, 140 000 ML and 300 000 ML; 130 K, 130 000 ML and 90 000 ML; 135 K, 150 000 ML and 190 000 ML; 140 K, 50 000 ML and 130 000 ML; 145 K, 100 000 ML. The ΔCPD curves shown have been scaled by the actual coverage divided by the target coverage.

The initial ΔCPD for growth above 120 K, though small, is not zero, nor is it even monotonically decreasing with temperature. This is somewhat suggested from Figure 4. The initial ΔCPD at the initial growth temperatures, from Figure 4, is plotted in Figure 5a. Here it is clearer that the ferroelectric effect shows a strong nonlinear decrease with temperature and shows some sign of a small maximum between 120 and 150 K.

The slight maximum between 120 and 150 K could be made much more apparent by using much thicker films. Shown in Figure 5b, this data makes it clear that the ΔCPD goes to a small but nonzero minimum near 130 K and that there is a clear local maximum at 140 K (again, the ΔCPD shown have been rescaled by the actual coverage divided by the targeted coverage, which was 150 000 ML). As will be discussed later, Su et al. observed their ferroelectric effect between 120 and 137 K, and mostly at the latter temperature, near the local maximum.[3] Above 140 K the ferroelectric effect rapidly declines, and by 150 K it appears to be zero, or at least 30-fold less than at the local minimum near 130 K. It is difficult to grow the ice films above 150 K in our apparatus owing to the increasing vapor pressure of the ice, so no higher temperature data are reported here. The data sets for the thick and thin films do not agree quantitatively on a per monolayer basis, where the data sets overlap. For example at 110 K the thick film gave about 32/150 000 V/ML, or about 0.21 mV/ML, while the thin film gave about 1.2/2000 V/ML = 0.6 mV/ML. This discrepancy is in large part expected to be caused by a nonzero intercept for the voltage versus coverage (−0.5 V was the offset at 40 K). Also, changes in the first monolayer work function change and residual contamination effects (discussed later) can add absolute uncertainties on the order of several tenths of a volt in the CPD.

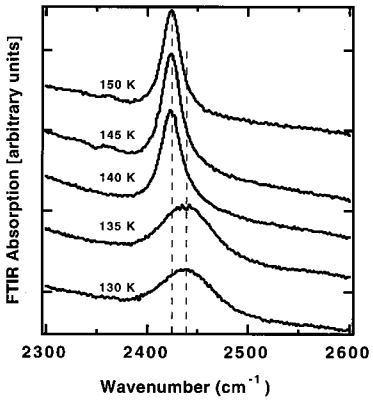

Figure 6. IR spectra of the decoupled OD stretch of HOD (∼1%) isolated in H_2O ice. Spectra were collected for ice grown at (bottom to top curves) 130 (a), 135 (b), 140 (c), 145 (d), and 150 K (e). Crystallization occurs between 135 and 140 K.

Together these will tend to increase the apparent ferroelectricity for thinner films and render the value more uncertain.

Somewhere above 120 K the vapor-deposited ice should become crystalline rather than amorphous.[17,18] While published studies are useful guides, the crystallization is a nonlinear kinetic process, and it would be best to know the actual crystallinity of ice grown under the same conditions as the films whose ferroelectric properties were measured. FTIR measurements have been shown to be a sensitive probe of crystallinity for water.[18] We matched the film growth rate and the delay between growing the film and measuring its FTIR spectra to those of the CPD measurements. The FTIR films were grown on a KBr substrate, not Pt(111). However for these thick films the state of the substrate seems to little alter the ferroelectric effect (as we later show, our results compare well with those of Kutzner[9]), and thus we suspect growth on KBr to not be much different than that on Pt(111) (however, substrate effects have been seen by some; see ref 18d). The FTIR lines of even crystalline ice are broad owing to the strongly coupled H-bonded network. But H_2O ice doped with a small amount of D_2O produces isolated HOD molecules whose vibrational lines are much narrower, as they are not degenerate with their neighbors. The OD stretch provided a narrow vibrational band at 2425 cm^{-1} that can be used to distinguish between sintered amorphous ice and crystalline ice.[18]

Figure 6 shows FTIR spectra of the 2425 cm^{-1} OD stretch in 1% D_2O-doped water. FTIR data were obtained from 120 to 150 K. Little change in peak shape or position was seen below 130 K. The breadth of this peak indicates the deposits are mostly amorphous at deposition temperatures below 135 K. At 135 K the peak is slightly narrowed, and by 140 K it is much narrower, nearly reaching the crystalline limit (exemplified by the 150 K spectra). For deposits at 145 and 150 K the peak width indicates that the ice film is completely crystallized within the 5 min since deposition. This is 10−15 K lower than where we see crystallization occur when a low-temperature deposit is warmed through this range at about 10 K/min.

Another spectral feature that is useful in characterizing the ice films is the stretching mode of OH groups that are not hydrogen-bonded to any oxygens.[18b] These are true dangling bonds and are associated with the surface, internal voids, etc. (these dangling bond states are not believed to be simple L-defects, as the latter would still be too strongly coupled to have this narrow a spectrum). As shown in the insert in Figure 7, these dangling bond OH stretch peaks are very narrow and are easy to see even at low concentration. Their prevalence

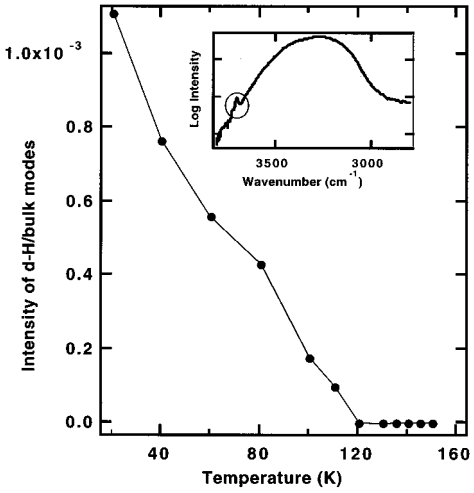

Figure 7. (Inset) shows the OH stretch band (for 40 K growth) and the small, narrow dangling OH feature. The ratio of the integrated IR intensity of the dangling OH surface groups divided by the integrated IR bands of the bulk OH stretch as a function of deposition temperature is plotted in the main figure.

can be estimated by simply taking the ratio of the narrow peak to the broad OH peak underlying it. This is plotted in Figure 7. They are rare even in the most amorphous ice deposited. The decrease in the ratio with increasing deposition temperature looks very much like the variation of the density of amorphous ice versus growth temperature curve reported by Brown et al.[19] The decrease in dangling bonds is fairly linear between 20 and 120 K. When the ice was grown at 20 K and warmed to a given temperature T_1 at 0.5 K/s (data not shown here), the dangling bond signal decreased more slowly than for films deposited at T_1. For example the dangling bond signal goes to zero for films *deposited* at 120 K. But when ice was deposited at 40 K and then ramped in temperature, the dangling bond signal disappears at about 130 K. The time decay of the integrated dangling OH FTIR intensity in ice films was recently reported for deposits made between 90 and 120 K over 25 min periods.[18c] However, we are most concerned with the ice film properties at 5 min after deposition.

Using very thick films as is done here makes it difficult to avoid contamination problems. A 150 000 ML film of water from a water doser that contributes 7 parts per million in the vapor phase of oxygen molecules (about 2×10^{-4} Torr partial pressure oxygen to water's 25 Torr vapor pressure) will contain 1 monolayer of oxygen molecules. Three cubic centimeters at 760 Torr of oxygen dissolves in 100 cm^3 of water at 25 °C, to give a 20 ppm liquid. To reduce the oxygen vapor level down to 7 ppm or 2×10^{-4} Torr requires a solution phase reduction by a factor of 4 million, or 5 ppt (part per trillion) water impurity oxygen. This is very hard to obtain with freeze−thaw treatments, and it still gives a full monolayer of oxygen. Even for 2000 ML films, it was difficult to avoid some contamination, as evidenced by its effect on our CPD runs. Oxygen has been shown to dissociate at 150 K on Pt(111), to yield tightly bound O atoms.[20a] This raises the work function and will also stabilize water coadsorbed via OH formation,[20b] to yield a TPD peak for water at higher temperature (∼215 K, with a long tail[20c]) than the typical water monolayer.[20b] This often causes complex work function changes of a magnitude of about 0.2−1 eV from 190 to 300 K.

Figure 8a shows the raw, unshifted CPD signals versus temperature for several nominal 2000 ML films, two deposited

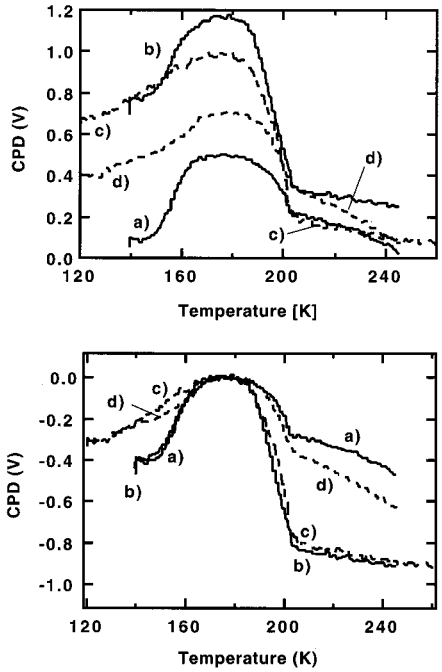

Figure 8. (a, b) trace a, 2200 ML, deposited at 140 K; trace b, 2300 ML at 140 K; trace c, 2000 ML at 120 K; trace d, 2300 ML at 120 K, where the differing temperature is the important variable. In (a, top), it can be seen that there is considerable scatter in the absolute CPD from run to run, owing to changing surface and probe conditions. However, note that by setting the traces to zero at 176 K, in (b, bottom) the runs deposited at the same temperature now overlap at temperatures below the water desorption. The differences after water desorption illustrate the work function of the clean Pt(111) (traces c and d) compared to the work function with oxygen present as a surface contaminant (traces a and b).

at 120 K and two at 140 K. All show several tenths of a volt shift, due probably in part to both some small amounts of persistent surface oxygen and some shifts of the gold-plated Kelvin probe. Traces a and b, for example, show continuous changes in the work function above 200 K, indicating that oxygen is present on the surface[20] (surface oxygen dissociatively binds water). Traces c and d show little sign of surface oxygen but show some offsets, probably from Kelvin probe contamination. Figure 8b shows the traces after shifting the data to correct for these effects. This is possible, as we found that by about 175 K, all ferroelectric voltages disappeared, and a flat-topped work function plateau occurred. By shifting the film voltages by subtracting their value near 175 K, we were able to eliminate most of the contamination effects upon the data for temperatures less than 175 K. Figure 8b shows how the runs at 120 K now agree closely with each other as to the ferroelectric effects *below* 175 K, as do the runs for ice grown at 140 K.

The behavior below 175 K after subtracting the 175 K values, and after rescaling by target coverage divided by the actual coverage (typically a 20−50% correction), gave ferroelectric voltages that were repeatable on the order of 0.1 V. However, it is not clear what fraction of the 0.6 eV CPD change due to the first monolayer is fully developed at the deposition temperature. Any evolution of this would look like a ferroelectric effect. To minimize this possible effect, and further suppress effects of ppm contaminants, we used much thicker films when the absolute film voltages became small. The 150 000 ML films had ferroelectric film voltages on the order of 10 V (except for 150 K grown ice, which was nearly zero), much larger than any residual contamination effects or first-monolayer effect.

Discussion

Our goal is to determine *quantitatively* the degree of polarization of the water molecules in the ice films. We should compare our ice polarization to a hypothetical basal-plane oriented ice, fully proton-ordered. How many millivolts per monolayer would that be? For cubic ice I that is perfectly polarized, assuming the nonorientational polarization of the ice molecules remains linear with the fields and is represented by the infinite frequency dielectric response of $\epsilon_\infty = 3.3$, the change in CPD for water at a surface concentration of 1.05×10^{19} m^{-2}, each with net dipole μ_z in the direction of the surface normal, is

$$\Delta\mathrm{CPD}_{\mathrm{pol}} = \frac{1.05 \times 10^{19}\ \mathrm{m}^{-2} \times \mu_z \times 3.33 \times 10^{-30}\ \mathrm{C\ m\ D}^{-1}}{\epsilon_0 \epsilon_\infty} \tag{7}$$

where ϵ_0 is the permittivity of vacuum and ϵ_∞ is the infinite frequency dielectric constant of ice (=3.3). To obtain the fraction of μ_0, the dipole of the water molecule in ice, which is aligned along the normal to the surface, we assume we have the basal plane of cubic ice I (cubic or hexagonal) exposed. Consistent with the tetragonally hydrogen-bonded water molecules, each water molecule has $\pm\mu_0/(3)^{1/2}$ aligned along the surface normal. Perfectly polarized ice would have all waters aligned to place the hydrogen end of the molecule as much toward the substrate as possible, giving a *z* component for each water dipole of $+\mu_0/(3)^{1/2}$. In the gas phase μ_0 is 1.9 D.[21] But in ice crystals, the electric dipole fields of neighboring water molecules stabilize the dipole even further and, through the polarizibility of the water, increase μ_0 to about 3.[21] By using the ϵ_∞ in the denominator of eq 3 with the 3.3 value, which implies no reorientation of water dipoles, we still are permitting the net dipole in the layer to be shielded owing to an induced polarization of the water molecules. This is questionable, and it may be that the better estimate is up to 3.3 times that of eq 3. The voltage per bilayer, with ϵ_∞ of 3.3, would be 2.1 V per monolayer of water. So when we observe about 3 mV/monolayer at 40 K, we have 0.003/2.1 = 0.15% of the field of a perfectly polarized ice crystal. We plot in Figure 9 the net aligned dipole per molecule versus ice growth temperature, which is the data from Figure 5 multiplied by (1.7 D)/(2.1 V/ML). Near 140 K, we do not plot the less accurate data from 2000 ML films but instead use the 150 000 ML film data.

The ferroelectric orientation per molecule we observe ranges from about 0.004 D to less than 0.000 01 D, a small effect. However, this small effect has some big implications for certain experiments, as discussed below.

It cannot be discerned from our work when we find, for example, 0.2% net polarization, if out of 1000 water molecules (a) 501 are oriented oxygen up and 499 oxygen down or (b) the crystal lattice is distorted so all the waters share in this net orientation equally or (c) 2 of the molecules are actually associated with polarized defects in an otherwise unpolarized crystal.

In 1972 Kutzner[9] published a paper on the spontaneous polarization of condensing gases with an electrical dipole moment. Included in that paper were data for water films formed in the temperature range of 3−110 K. By scanning and digitizing this previously published data, and converting their reported measured parameters, $I_g/(\mathrm{d}M/\delta t)$ (where I_g is the current to a plate condensing ice and M is the amount of water vapor deposited in Torr·L/s), to that of an electrical dipole moment per molecule, we are able to compare our data with that work. We used the conversion equation given by Kutzner[11]

$$\bar{\mu} = -\left(1.14 \times 10^8\ \mathrm{D}\ \frac{\mathrm{Torr \cdot L}}{\mathrm{A\ s}}\right)\left(\frac{I_g}{(\mathrm{d}M/\mathrm{d}t)}\right) \tag{4}$$

where we have substituted into his equation $\epsilon = 3.3$ for water below 80 K and spacing $d = 0.4$ cm (for the Kutzner experiments). Figure 9 shows a plot of the mean surface normal aligned dipole moment per molecule, μ_z, as a function of the deposition temperature, from Kutzner's data. In that plot we compare our data (open circles) to that of Kutzner's (the dotted line) and find that we have agreement within experimental error in the low-temperature region up to about 90 K. In the range from 90 to 150 K, we observe some significant phenomena that require very thick films to ensure a measurable surface potential when μ is extremely small. With very thick films we are able to observe changes in a very small dipole moment with a precision far higher than that obtained previously, and it is in that range that our data significantly diverges from the data reported by Kutzner.

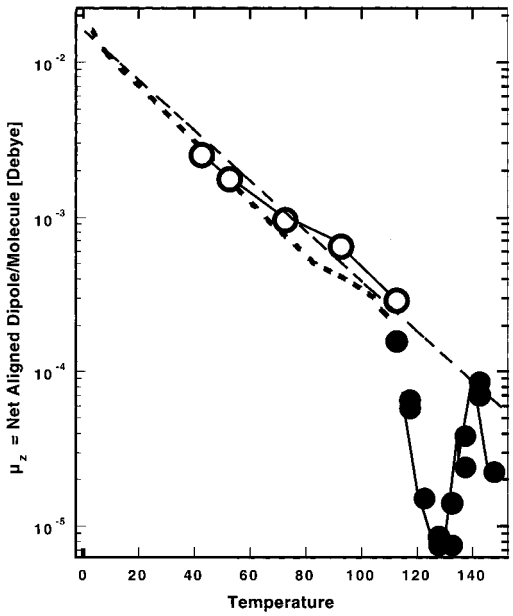

Figure 9. Net oriented dipole per molecule (in D) as a function of deposition temperature. The open circles are for films of about 2000 ML, and the solid circles are for 2 orders of magnitude thicker films. (When the mean dipole moment per molecule drops below 10^{-4} D, the measurements require very thick films to get significant results.) The heavy dashed line represents the Kutzner data[9] calculated from his plot. The thin dashed line is an exponential fit. Multiplied by (2.1 V/ML)/(1.7 D) the vertical axis gives the voltage per monolayer, and divided by (1.7 D) gives the fraction of maximum alignment.

The net polarization of the ice films tends to disappear when one either grows the ice at progressively higher temperature or heats a film grown at low temperature to higher temperatures. One mechanism for this to happen is via the ice's dielectric constant, which upon becoming fully active at higher temperature may be able to shield the external field produced by any polarization. Alternatively, of course, the polarization itself can be disappearing. One might suppose that these two options were the same, as ice only has a high dielectric constant (in the absence of free carriers) because of the reorientation of water molecules, thus creating less polarization. But the distinction can make sense, for example, if the initial polarization is caused by a defect. The defect could disappear at a lower temperature than where the dielectric constant turns on, or the defects could

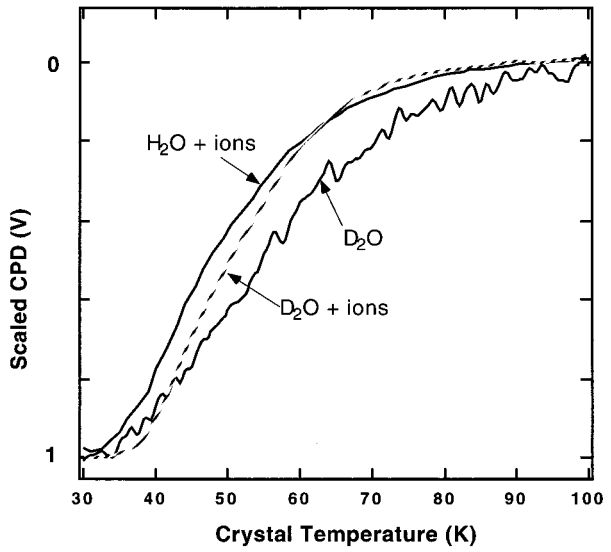

Figure 10. Decay of the ferroelectric voltage as ice film is warmed above the 27 K growth temperature compared to irreversible dielectric turn-on of amorphous ice plus ions. Data were rescaled and inverted as necessary, to compare shapes. H_2O film had initial film voltage from ions (Cs^+ ion deposition) of about 3 V for the 60 ML film. D_2O + Cs^+ ion film is an 80 ML film, 6.5 V film voltage, and a 0.5 K/s ramp. D_2O film ferroelectric voltage (−0.9 V) is for 80 ML film, ramped at 0.166 K/min.

persist past the temperature where (most of) their field is shielded by the dielectric constant.

We have studied thin film ice's dielectric properties for separate publication.[13,22] In one study, we showed, using soft-landed ions, that amorphous water's dielectric constant turns on any time it is heated for the first time to a temperature higher than it has been heated to before, from 30 K up to about 120 K.[22a] This is due to stress-induced relaxation of the "fluffy" amorphous ice, which creates an irreversible polarization in the presence of a preexisting electric field. The amount of such data available for H_2O is less than that for D_2O, and the best comparison between this irreversible dielectric turn-on and the ferroelectric effect can be made for D_2O data. Figure 10 shows a D_2O film deposited at 27 K displaying an initial ferroelectric film voltage, as well as a D_2O film and an H_2O film both initially biased with Cs^+ ions. As the temperature is ramped, all the films show a similar drop in film voltage magnitude, but the ferroelectric film curve seems to have a slightly slower decay. While the differences could be attributed to many things (e.g., field strength effect,[22b] details of the local geometry playing a role in permitting dielectric screening), the curves are more alike than different. 90 K grown films show a depolarization upon heating also very similar to the behavior of ion-dosed ice.

We now discuss the growth temperature dependence of the ferroelectric effect. The FTIR data in Figure 7 shows a roughly linear decrease in intensity of the dangling O−H groups to zero near 120 K, very similar to that seen in Figure 5a for the ΔCPD data, and the two graphs even have about the same absolute scales on a per monolayer basis (see Figure 9 for scale). But a linear change in water's density from about 0.6 g cm^{-3} to a limiting value of 0.9 g cm^{-3} near 120 K is also seen for amorphous water versus growth temperature, as measured recently by Brown et al.[19] This means there is a lot happening in amorphous ice over this temperature range, so it might be that both the dangling bond states and the ferroelectric ordering may be the results of a more basic cause.

The ferroelectric effect looks rather linear in the log plot of Figure 9, except for the sharp dips near 130 and 150 K. Shown in that figure is a linear fit to the data, which shows the ferroelectric effect in terms of net aligned dipole moment per molecule is roughly (0.016 D)·exp(−T/27 K).

The FTIR data shows that the water is just beginning to grow crystalline at 135 K and is nearly fully crystallized when grown at 140 K. One might suppose this would cause a large change in ferroelectricity. It does, but the effect is that the ferroelectricity is restored to the value extrapolated from the data from temperatures lower than the 130 K minimum.

Exponentials in T are not commonly seen in experiments: typically seen are exponentials in 1/T. We have no confirmed model for this. We did construct a simple model that does fit the data well and is at least partly physically plausible (in predicting the rapid drops in ferroelectric effects near 120 and 145 K). But it is in part rather speculative, too. One can suppose that the molecules as they adsorb locally have some initial inherent preference to slightly align ferroelectrically. This effect is destroyed by heating, either by "annealing", by removing defects that create the ferroelectric field, or by activating the local dielectric constant, which would then shield the fields of the polarization. We suppose that this process follows an Arrhenius rate versus temperature (preexponential c, activation energy E_a) and that there are two temperatures and two time frames for this process. One is the time Δt_1 spent at the growth temperature T_g. The second involves a local rise in temperature caused by the heat of condensation of individual molecules. This causes a warming of the ice from the growth temperature T_g by a δT, for depth of several layers, for some number of picoseconds Δt_2. Because the stressed ice is a rather metastable system, this local energy release upon adsorption can cause significant effects that would not be there if the adsorption was that for an equilibrium solid. The two annealings can be expressed as two rates pushing the dielectric response (or ferroelectric loss) toward equilibrium. This allows an estimate of the effect to be made via eq 5:

$$\text{net aligned dipole} = \frac{((0.016\ \text{D})\cdot 3.3}{3.3 + \epsilon_z^{-E_a/(RT_g)}\,(1 - e^a)} \qquad (5a)$$

$$a = \sum_j \Delta t_j k_j = (300\ \text{s})\cdot c e^{-E_a/(RT_g)} + \Delta t_2 \cdot^{-E_a/(R(T_g+\delta T))} \qquad (5b)$$

ϵ_z is the zero-frequency dielectric constant, and eq 5b gives the contribution to the t/τ from both the temporary heating around an adsorbing molecule and the effect of the 5 min from growth to measurement. If the loss of original polarization dominates over dielectric response, the fitted ϵ will be larger than the expected 200 or so. Use of the same Arrhenius kinetics for both processes is reasonable, as both can be due to the same mechanism, the generation of L and D defects in ice (many transport and dielectric properties of ices have similar or identical activation energies, which is often attributed to common mechanisms[17]).

If one restricts the fit to exclude the region above 130 K, thus fitting only the amorphous ice part of the data, one gets the fit shown in Figure 11. The fit was done directly in the log form, to give more weight to the higher temperature part of the curve. The fits could tolerate a very wide range of some variables, like ν and Δt, so we decided to fix one on the basis of physical ideas. The δT fitted were roughly 340 ± 50 K. The dT of 340 K can give an independent estimate for the time Δt. If we assume that the heat dumped locally is the same as the heat of evaporation used in the water desorption kinetics, 48.25 kJ/mol,[12] with a heat capacity of ice of 0.2 cal/K/g at

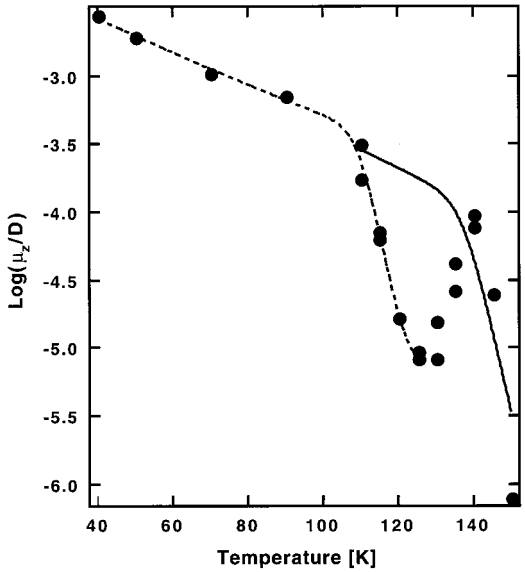

Figure 11. Measured ferroelectric effect compared to a simple annealing/relaxation model, for crystalline ice (solid curve) and for amorphous ice (dashed curve).

TABLE 1: Parameters for Fitting *T*-Behavior of Ferroelectricity

	amorphous ice (≤130 K region)	crystalline ice (115−150 K minus dip)
c	1.1×10^{15} s^{-1}	1.7×10^{15} s^{-1}
E_a	41 kJ/mol = 0.43 eV	54 kJ/mol = 0.56 eV
δT	340 K	340 K (fixed from amorphous fit)
ϵ_z	23 000	6100
Δt	1 ps (fixed)	1 ps (fixed)

110 K[23] (not highly temperature dependent) and an average density of ice of 0.8 g/cm^3, then the dT of 340K implies a region heated of a cube about 7 Å on a side. This distance scale allows an estimate of the time to cool, as Δt_2 should be roughly equal to (7 Å)·(7 Å)·(heat capacity)/(thermal conductivity), where the heat capacity is per unit volume. For the thermal conductivity of 5×10^{-3} W/cm/K and a heat capacity of 0.7 J K^{-1}cm^{-3}, this gives a Δt_2 of 0.7 ps. We rounded this off to a *fixed* Δt_2 of 1 ps. The refitted parameters now appear in Table 1 and the fit in Figure 11. To use eq 5a to fit the data for crystalline ice is not so easy, as only a few points from 140 to 150 K exist. It is not unreasonable to assume that, at lower temperatures, the crystalline results might have resembled the amorphous results (below the "dip region" at 130 K) had crystalline ice been able to grow at low temperatures. Accordingly, we add one amorphous ice data point from 115 K to the "crystalline" ice data subset. As the thermal properties of crystalline and amorphous ice are similar, we further fix dT to be 337 K. Then the best fit results for crystalline ice are also shown in Figure 11 and Table 1.

The activation energy of 0.56 eV is very similar to the activation energy normally seen for crystalline ice (0.56−0.59 eV[17]). Moreover, the fitted $c = 1.7 \times 10^{15}$ s^{-1} matches the expected value for water ice. For example, using it and the exponential in E_a, we calculate, at 273 K, a $t = 1/k$ of 20 μs, in agreement with ref 17. If we had simply used the literature values for c and E_a, we would have fit the data with only two independent parameters, ϵ_z and dT. However, the fitted ϵ_z's are much bigger than 200, implying (to the extent the model is valid) that the polarization itself disappears; it is not just dielectrically shielded. That the amorphous ice has a dielectric constant that has a shorter relaxation time (and thus temperature) than crystalline ice is well-known,[24] and it should be active just in the same temperature range as the first decrease near 120 K.

Admittedly the model and fit above are rather speculative, especially with respect to the local transient heating effect. But nonetheless the fitted parameters make good physical sense.

It is instructive to see if the dips near 130 and 150 K can be attributed solely to an increase in the dielectric constant near those temperatures (above we showed that the *full-range* temperature behavior of the ferroelectric effect is too large to be attributed to just dielectric screening). If we extrapolate the linear fit in Figure 9 to the position of the minimum ferroelectric alignment at 130 K, the result is 1.3×10^{-4} D. We observed 8×10^{-6} D. This reduction is by a factor of 15 and should equal the ratio of the dielectric constants. The span between 3.3 and 200, roughly the high-frequency and zero-frequency limits of the dielectric constant at that temperature, is larger than that ratio, so it is possible the dip at 120 is due to dielectric screening and not loss of the alignment.

Over the years there have been many UFI citings (underidentified ferroelectric ices) in the literature regarding ice I, often where the hope was high, and the data suggestive, that a fully proton-ordered ice phase was created. This work falls roughly in this category, as while the ice is clearly ferroelectric, it is only feebly aligned. The proper perspective comes from quantitative assessment of the alignment. We discuss recent work by Su et al.[3] and Whitworth and co-workers[67] to examine how proton-ordered their materials might be.

Su et al.'s very recent ferroelectric ice observations can be possibly explained by the same weak ferroelectric effect we see in ref 3. They do not in their paper discuss how aligned their ice is, or would have to be, to produce the sum frequency signals they observe. Despite this, many reading it have thought they meant it was fully proton-ordered. We believe it is only very slightly ordered. They observe films grown at 137 K, or films grown at 120 K and then annealed at 137 K. That the SFG signal could be due to a small ferroelectric potential on order of a fraction of a millivolt per monolayer (what one would expect from 120 to 137 K from our results) is supported by analogous experience in second harmonic generation (SHG) signals near electrified interfaces. Some recent work by Zhao et al.[25] illustrates this point. In that work they found for the interface between electrolytic solutions and air, the SHG signal from those molecules directly at the air−electrolyte interface was small compared to the signal from the adjacent bulk double-layer region. There is a potential difference between the interface and the bulk solvent created by the loss of inversion symmetry. This generated a dominating nonlinear optical signal in the water, from the potential differences ranging from 10 to 150 mV. The potential gradient extends across the hundreds-of-angstroms scale of the electrochemical double layers that exist at the electrolyte−air interface. They show that only the potential difference, not the distance over which it occurs, is important. If we use our results for a 140 K grown ice, Su et al. should have about 10^{-4} V/ML ·30 ML = 3 mV ferroelectric potential difference. It would appear from their data that the alignment might be severalfold higher in the first 30 ML, so this might generate 10 or more mV for the 30 ML film. This is the same order of potential difference that created a dominating SHG for Zhao et al. Thus we suggest that a small ferroelectric effect on order of 10^{-4} aligned dipoles could account for the SFG signal seen by Su et al.,[3] and so, a completely polarized ice film is not indicated by their data.

It could be that the ferroelectric effect that we identified as a true bulk effect at 40 K via coverage plots such as Figure 3

may not be bulk effects at all temperatures. We do not have volts versus coverage curves for many temperatures. For example, what if the 16 V film voltages we see from 150 000 ML films grown at 140 K was actually due to the first 30 ML being 50% polarized and the remaining film being unpolarized. At about 2.1 V/ML for fully polarized ice, this would be expected. However, at 140 K we do have data at two coverages: 2000 and 150 000 ML. The 2000 ML film (Figure 5a) gave −0.4 V and the 150 000 ML film −16 V. These numbers are not in strict linearity with coverage (small offset voltages, first monolayer, and contamination effects limit the small voltage accuracy, as discussed earlier). But the results clearly show that the first 30 ML or so cannot be highly aligned. We can say that at 140 K it is unlikely that the first 2000 ML are more polarized than ((0.4 V)/2000 ML)/(2.1 V/ML) = 0.01%, and the first 30 ML not more than ((0.4 V)/30 ML)/(2.1 V/ML) = 0.6%.

The analysis above and our results make it plausible that Su et al.[3] see only a very small net orientation (with net oxygen up), and they provide no quantitative claim to the contrary to our assertion. This conclusion is further supported by evidence long in the literature. If the first 30 monolayers were largely proton-aligned, the work function would necessarily change with coverage at about 2.1 V/ML, for a total change on order of 63 V. But published work function measurements up to about 5 ML (under somewhat different conditions) show that the total work function change at 5 ML is only about 1 eV total and is nearing an asymptotic limit.[26] As mentioned above we have looked at work function changes at and near 140 K many times, for these ferroelectric studies and for soft-landing ion experiments[22] from 30 to 100 ML. We clearly saw that no large polarization exists for the first 30 ML. In work to be published, we report that the ferroelectric effect is constant per monolayer near 40 K, from 5 to 2000 ML,[27] with net O out.

Ice doped with hydroxide shows dielectric activity down to about 70 K, below which the temperature-dependent response time is too slow for convenient laboratory studies.[5] This catalyzed behavior is clearly intriguing. Whitworth and co-workers suspect proton ordering in this system is possible since both achieving proton order and high dielectric response require flipping orientations of water molecules,[17] which the hydroxide clearly catalyzes. They start with 0.055 M KOH solutions and freeze them. They see phase separations on a microscopic scale, and they presumably form ices with a wide range of dissolved hydroxide concentrations, from near zero to hydrated KOH. They term the ice formed, or at least some of the ice formed, as "ice XI", which they conclude is a proton-ordered version of ice I, which they also claim is ferroelectric. The ice XI studies involve holding ice samples for long periods of time at temperatures just below where the dielectric constant response time slows down to many seconds or hours, while under a bias. They are then studied by stimulated depolarization spectroscopy, where the field is removed, the ice is slowly warmed, and the currents generated at zero bias are recorded. These ices have also been studied by neutron diffraction.[7] These diffraction studies, while "sensitive" to proton-order, will produce fine diffraction even when completely proton-disordered. They see new diffraction spots for this system, which they assign to a unit cell that could be ferroelectric and might reflect proton order, though it could also reflect oxygen motions and may involve hydroxide−water superlattices.

If their ice XI phase was ferroelectric (aligned) versus antiferroelectric (alternating), it might be detectable via its electric properties. Ferroelectric phases are difficult to identify, owing to hysteresis effects and expected fine-grain structure of differing alignments. An excellent discussion of these issues was made by Johari and Jones.[8] They discuss the earlier work[4] where Dengel et al. claimed to have seen a ferroelectric ice transition in ice I near 100 K. Most water experts are now convinced that Dengel et al.'s observations, which they interpreted as phase transitions, were simply a kinetic hysteresis effect of the dielectric response. This created transients both in heat capacity measurements and thermal depolarization spectroscopy. Johari and Jones do an excellent job of showing how the known kinetics would reproduce Dengel et al.'s electrical effects quantitatively. They show how a biased material, held for hours just below the temperature where the dielectric constant conveniently responds, will polarize slowly with a normal, nonferroelectric dielectric constant. And upon warming, it will release that polarization over a fairly narrow temperature range, when the dielectric kinetics finally begin to respond in a minute time frame.

What is striking is the similarity between the observations and methods of Whitworth and co-workers[6] and those of Dengel et al.[4] Because of the effectiveness of hydroxide as a catalyst for the dielectric activity, we would expect the system of Whitworth and co-workers to show electrical hysteresis effects near 70 K, where for the more sluggish ice of Dengel et al., around 100 K is needed. The simplest conclusion would be that the electrical studies of Whitworth and co-workers do not suggest a ferroelectric phase transition at all and are just the expected results of hysteresis in the sluggish dielectric response.

Are the results of Jackson and Whitworth[6] quantitatively consistent with a sluggish, simple, dielectric polarization ("electret effect") or a true ferroelectric transition? Ferroelectric materials show a dielectric behavior that goes as $C/(T - T_0)$, where T_0 is the ferroelectric phase transition temperature.[28] This is true on either side of T_0. Ice XI is supposed to actually make this transition near 70 K,[6,7] involving a large fraction of the material, per the neutron diffraction results. If true, then the dielectric constant should grow very, very large around 70 K. We can numerically analyze their data to assess this (with limited accuracy). First, how polarized is the ice in their study? They apply gold electrodes to an ice sample of 2 cm × 1.4 cm × 0.2 cm thick. If at any time they had 100% aligned ferroelectric ice, then the potential difference across a 0.2 cm plate (assuming the electric field is perpendicular to the face) will be 2.1 V per monolayer thickness, or 2.1 V·(0.2 cm/3 × 10^{-8} cm) = 130 000 000 V (!!). This they do not see (nor claim), as the material should adopt a grain structure of largely counteraligned ferroelectric domains. To assess the dielectric constant, one can use the current they sensed with an electrometer, for zero bias across the electrodes. The charge collected should be the voltage divided by the capacitance of the ice film. Since a fully polarized, single domain material should have only a dielectric constant of near 3.3, the capacitance should be

$$C = 0.02\ \text{m} \cdot 0.014\ \text{m}/0.002\ \text{m} \cdot 3.3 \cdot 8.8 \times 10^{-12}\ \text{F/m} = 4\ \text{pF} \quad (11)$$

This would give a charge of 130 000 000 V·4 pF or 520 μC. They observed a maximum charge of 1.2 μC dumped during the return of ice XI to normal ice upon heating, at zero bias.[6] This would suggest that they were at most 1.2/520 aligned or 0.002. The dielectric constant they see can be calculated as 1.2 μC/420 V, or 2900 pF. This means their dielectric constant should be about 2900 pF/4 pF, or 680. They bias the ice for many hours several degrees below 70 K. Their hydroxide-catalyzed dielectric response is active down to about 70 K (in

the 10 s time domain) but could well be fully active for the long times they use, slightly below 70 K. Ordinary ice's dielectric constant goes nearly as (27 000 K/T) when active, which would be about 390. So our estimate (using the published geometry) shows that ice XI shows no more than a factor of 1.7 times the value expected for nonferroelectric ice, and they may well be equivalent, given the limited information. What is very clear is that no extreme increase in dielectric constant ($C/(T - T_0)$ with T_0 near 70 K) is seen in the material as it changes to and from ice XI. This eliminates any possibility that the transition they see is ferroelectric in nature. What is seen electrically is consistent with kinetic hysteresis effects on the ordinary dielectrically stored charge being released around 72 K, when the response time of the dielectric constant becomes short enough. One could be more comfortable with an antiferroelectric ordering occurring near 70, but they argue this is not possible from the unit cell symmetry via the neutron studies.[7]

A further caution is to note that in any sort of depolarization experiments, one might accidentally build up ferroelectric films on the outer surfaces of their ice sample or electrodes, especially during initial cool-downs. Water vapor from a part of the system not yet fully cooled can transfer quickly to the colder sections. At 10^{-6} Torr it will deposit around a monolayer every second. These could discharge upon heating, producing currents mistakenly attributed to the bulk ice.

Even though the ferroelectric effects we measure are small, they can have big influences under some circumstances. These effects are important to the experimental scientist interested in studying or using an ice layer. This is definitely the case for our experiments on the soft-landing of ions on ice films, to recreate electrochemical double layers in a vacuum, for example. At 40 K, a 100 ML film has about 0.3 V across it from the ferroelectric effect, which creates "offset effects" when dropping ions on top to reach certain desired voltages.[22] And it is certainly a major issue when employing nonlinear optical methods to study ice interfaces. Another experiment that is at least modestly affected by this ferroelectric effect is in the study of electron-driven chemistry on ice films, as done by Sanche, Orlando, and co-workers.[29] Alerted to this ferroelectricity through discussions with us, they show how it has some modest effects on kinetic energies of departing ejected ions, for example.

The study of ice formation on dust particles has long been a concern of atmospheric scientists. However, because of the temperature range of our experiments (30−150 K) and the fact that most atmospheric temperatures are in the range of 180−300 K, it is not likely that our work is relevant to those concerns. In space, though, ice forms from the vapor in molecular clouds, in solar nebulae, and on frigid moons and planets, under conditions that our data shows (at least at laboratory conditions) should produce ferroelectric ice.[30] A 1 km chunk of ice growing at 70 K should be about 10^{13} monolayers thick. At 1 mV/ML this is 10 000 000 000 V of potential between the inside and the outside! Millimeter particles should correspondingly have 10 000 V of charge. This potential can lead to net charging, and the resulting electrostatic repulsion between ice particles then could affect the agglomeration of, and chemistry within, ice particles in space.

Conclusions

We have observed a slight bulk ferroelectricity in vapor-deposited water. We believe it grows metastably during growth owing to the aligning influences of the inherently asymmetric solid-vacuum interface, and that it is independent of any substrate effects. For thicknesses up to roughly 100 μm, the ferroelectric voltage increased linearly with thickness, giving no indication of reaching any limit. Further, ferroelectricity was observed in films grown at as high a temperature as 145 K, where the ice film is almost entirely crystalline, but the effect is much more pronounced in films grown at low temperatures.

Near absolute zero we project that there would be about 1% of the water ice dipoles spontaneously aligned during growth. As the growth temperature increases, the ferroelectric effect decreases with an approximate exponential decline with temperature, which is consistent with a model where the heat of condensation of a water molecule causes a local annealing of the growing ice, thus reducing the net polarization. Near 125 K[24] the dielectric properties of amorphous water can respond in the 5 min of our experiment, masking the ferroelectric effect but not eliminating it. By 135 K the ice begins to grow crystalline. The ferroelectric effect reappears, as crystalline ice has a dielectric constant that is not active below about 145 K. The ferroelectric orientation itself seems to disappear at 150 K.

We see our slight ferroelectric ordering, perhaps slightly increased in the first 30 monolayers, being consistent with Su et al.'s[3] report of ferroelectrically aligned ice measured via SFG. We discuss the alignment in "ice XI", a reportedly ferroelectric ice I,[8] and suggest caution in interpreting their results as *ferroelectrically* proton-ordered ice.

Acknowledgment. Funding was provided by the Offices of Chemical Sciences and Materials Sciences, of the Basic Energy Sciences Division of the Department of Energy. Pacific Northwest National Laboratory is a multiprogram national laboratory operated by Battelle Memorial Institute for the Department of Energy under contract No. DE-AC06-76L0-1830. Helpful discussions were had with J. Devlin, V. Petrenko, T. Orlando, B.D. Kay, and others.

References and Notes

(1) Lekner, J. *Physica B* **1997**, *240*, 263.
(2) Pitzer, K. S.; Polissar, J. *J. Phys. Chem.* **1956**, *60*, 1140.
(3) Su, X.; Lianos, L.; Shen, Y. R.; Somorjai, G. A. *Phys. Rev. Lett.* **1998**, *80*, 1533.
(4) Dengel, O.; Eckener, U.; Plitz, H.; Riehl, N. *Phys. Lett.* **1964**, *9*, 291.
(5) Kawada, S. J. *J. Phys. Soc. Jpn.* **1972**, *32*, 1442. Tajima, Y.; Matsuo, T.; Suga, H. *J. Phys. Chem. Solids* **1984**, *45*, 1135.
(6) Jackson, S. M.; Whitworth, R. W. *J. Phys. B* **1997**, *101*, 7177. Jackson, S. M.; Whitworth, R. W. *J. Chem. Phys.* **1995**, *103*, 7646.
(7) Howe, R.; Whitworth, R. W. *J. Chem. Phys.* **1990**, *90*, 4450. Jackson, S. M.; Nield, V. M.; Whitworth, R. W.; Oguro, M.; Wilson, C. C. *J. Phys. Chem. B* **1997**, *101*, 6142.
(8) Johari, G. P.; Jones, S. J. *J. Chem. Phys.* **1975**, *62*, 4213.
(9) Kutzner, K. *Thin Solid Films* **1972**, *14*, 49.
(10) Onsager, L.; Staebler, D. L.; Mascarenhas, S. *J. Chem. Phys.* **1978**, *68*, 3823.
(11) The coverages of water (crystalline or amorphous) are given in terms of monolayers (ML), being the saturated crystalline "bilayer" of the water adsorbate. This is 1.05×10^{15} water molecules/cm^2. The Pt(111) surface has an atom density of 1.5×10^{15} /cm^2 and a spacing between bilayers of 0.38 nm. See ref 15.
(12) Speedy, R. J.; Debenedetti, P. G.; Smith, R. S.; Huang, C.; Kay, B. D. *J. Chem. Phys.* **1996**, *105*, 240.
(13) (a) Biesecker, J. P.; Ellison, G. B.; Wang, H.; Iedema, M. J.; Tsekouras, A. A.; Cowin, J. P. *Rev. Sci. Instrum.* **1998**, *69*, 485. (b) Tsekouras, A. A.; Iedema, M. J.; Ellison, G. B.; Cowin, J. P. *Int J. Mass Spectrosc. Ion Processes* **1998**, *174*, 219.
(14) Groner, P.; Stolkin, I. H.; Gunthard, H. *J. Phys. E* **1973**, *6*, 122.
(15) Thiel, P. A.; Madey, T. E. *Surf. Sci. Rep.* **1987**, *7*, 211.
(16) The tube doser's irreproducibility caused the actual coverages (determined by the TPD peak temperature) to vary from 1800 to 2600 ML. The ΔCPD shown have been scaled by the actual coverage divided by the targeted coverage of 2000 ML. As Figure 3 shows, the ferroelectric linearity tends to involve a small offset. We ignored this in this correction, a small error.
(17) Hobbs, P. V. *Ice Physics*; Clarendon Press: Oxford, 1974; p 92.

(18) (a) Buch, V.; Delzeit, L.; Blackledge, C.; Devlin, J. P. *J. Phys. Chem.* **1996**, *100*, 3732. (b) Buch, V.; Devlin, J. P. *J. Chem. Phys.* **1991**, *94*, 4091. (c) Zondlo, M. A.; Onasch, T. B.; Warshawsky, M. S.; Tolbert, M. A.; Mallick, G.; Arentz, P.; Robinson, M. S. *J. Phys. Chem.* **1997**, *101*, 10887. (d) Trakhtenberg, S.; Naaman, R.; Cohen, S. R.; Benjamin, I. *J. Phys. Chem. B* **1997**, *101*, 5172.

(19) Brown, D. E.; George, S. M.; Huang, C.; Wong, E. K. L.; Rider, K. B.; Smith, R. S.; Kay, B. D. *J. Phys. Chem.* **1996**, *100*, 4988.

(20) (a) Gland, J. L.; Sexton, B. A.; Fisher, G. B. *Surf. Sci.* **1980**, *95*, 587. (b) Fisher, G. B.; Sexton, B. A. *Phys. Rev. Lett.* **1980**, *44*, 683. (c) Fisher, G. B.; Gland, J. L. *Surf. Sci.* **1980**, *94*, 446.

(21) Burnham, C. J.; Li, J.-C.; Leslie, M. *J. Phys. Chem. B* **1997**, *101*, 6192 and references therein.

(22) (a) Tsekouras, A. A.; Iedema, M. J.; Cowin, J. P. *Phys. Rev. Lett.* **1998**, *80*, 5798. (b) Iedema, M. J.; Cowin, J. P.; Tsekouras, A. A., in preparation.

(23) Weast, R. C., Lide, D. C., Eds. *Handbook of Chemistry and Physics*, 70th ed.; CRC Press: Boca Raton, FL, 1989; p D-174.

(24) Johari, G. P. *J. Chem. Phys.* **1996**, *105*, 7079. Fisher, M.; Devlin, J. P. *J. Phys. Chem.* **1995**, *99*, 11584. Johari, G. P.; Hallbruker, A.; Mayer, E. *J. Chem. Phys.* **1991**, *95*, 2955.

(25) Zhao, X.; Ong, S.; Eisenthal, K. B. *Chem. Phys. Lett.* **1993**, *202*, 513.

(26) Kiskinova, M.; Pirug, G.; Bonzel, H. P. *Surf. Sci.* **1985**, *150*, 319. Kizhakevariam, N.; Jiang, X.; Weaver, M. J. *J. Chem. Phys.* **1994**, *100*, 6750.

(27) Wu, K.; Iedema, M. J.; Tsekouras, A. A.; Cowin, J. P. To be published.

(28) Jona, F.; Shirane, G. *Ferroelectric Crystals*; Dover Publications: New York, 1993.

(29) Simpson, W. C.; Orlando, T. M.; Parenteau, L.; Nagesha, K.; Sanche, L. *J. Chem. Phys.* **1998**, *108*, 5027.

(30) Kouchi, A.; Yamamoto, T.; Kozasa, T.; Kuroda, T.; Greenberg, J. M. *Astron. Astrophys.* **1994**, *290*, 1009.